Electronic Supplementary Material (ESI) for Physical Chemistry Chemical Physics.

Adatom Surface Diffusion of Catalytic Metals on the Anatase TiO_2 (101) Surface

Afnan Alghannam, [1] Christopher L. Muhich, [1,† *], Charles B. Musgrave[1,2]

[1]*Department of Chemical and Biological Engineering, University of Colorado, Boulder, Colorado 80309-5096*
[2]*Department of Chemistry and Biochemistry, University of Colorado, Boulder, Colorado 80309*
[†]*Present address: Department of Mechanical and Process Engineering, ETH, 8092 Zürich, Switzerland*
[*] To whom correspondence should be addressed e*mail: Christopher.muhich@colorado.edu*

Supporting Information

SI.1 Bond length as indicator of bond strength

The same trend of increased surface bonding leading to lower activation barriers is indicated by the predicted bond lengths. The activation barriers decrease as the number of nearest neighbors increase, which is correlated to the adatom-surface atom distance where shorter lengths indicate stronger binding. A greater number of bonds leads to a more stabilized TS and thus a lower activation barrier. Diffusion along Path 2 allows the adatom significantly more atoms to bond with than along Paths 1 and 3 because the adatom partially embeds itself into the surface, and hence interacts with more atoms than when the adatom diffuses on the surface. We illustrate this by comparing Fe adatom migration along Paths 1 and 2. The bond lengths of Fe-O_{2c}, and Fe-O_{3c}, at the TS of Path 2 are 1.77, and 2.14, respectively. However, at the TS along Path 1, Fe only bonds to one O_{2c} atom with a bond length of 1.85 Å. This leads to a higher stabilization of the Fe atom at the TS along Path 2 than Path 1 when comparing them to the OO site and therefore a lower activation barrier for diffusion along Path 2. This is also the case for other adatoms as shown in SI Figures 1-7, where a clear trend exists between the activation energy and coordination, with relative barriers of Path 2 < Path 1 < Path 3, with the exception of Au.

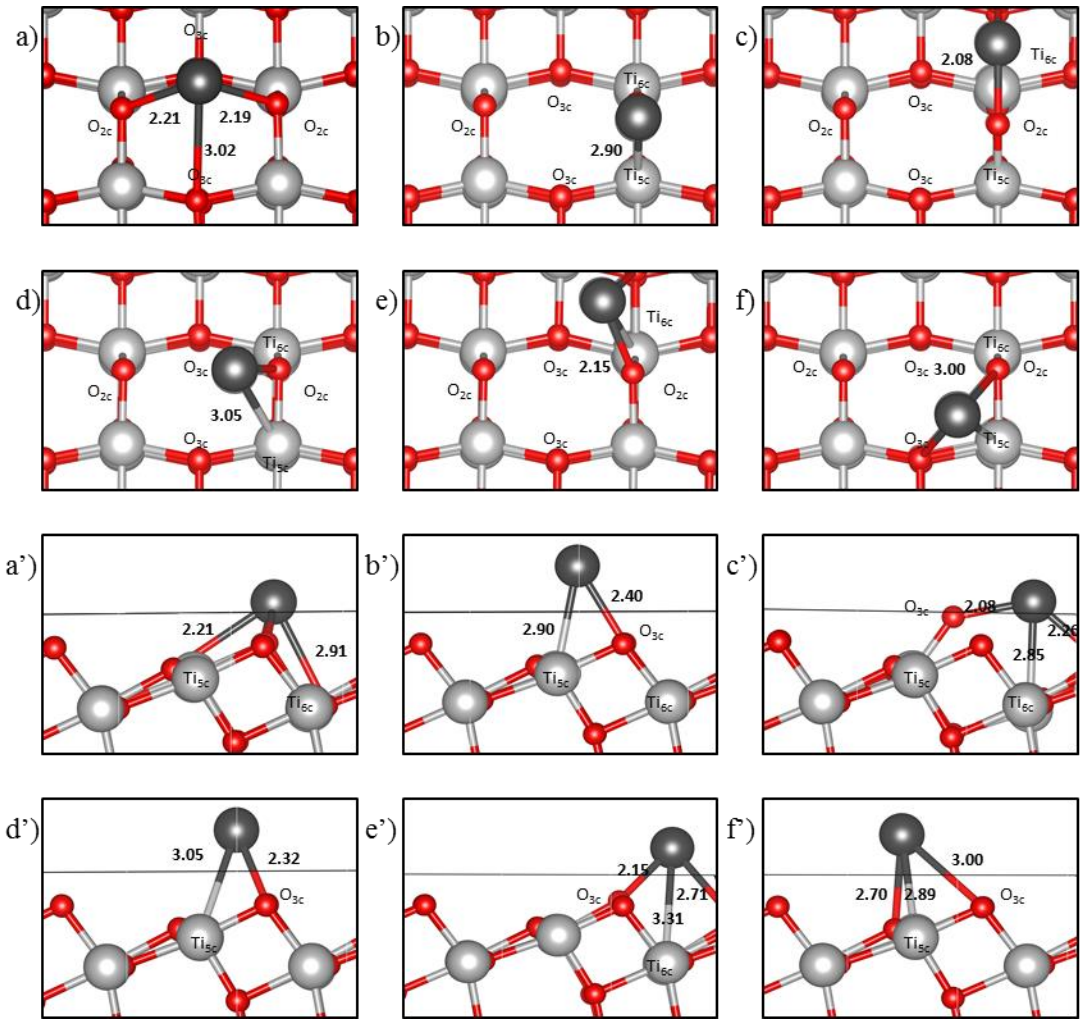

Figure SI: Top views of optimized geometries of a Ag adatom on Anatase TiO_2 (101) surface with bond lengths (in Angstroms): a) OO, b) OTi, c) OTiO. Rate determining transition state of d) Path 1, e) Path 2 and f) Path 3. The corresponding side views are shown in a'), b'), c'), d') e') and f').

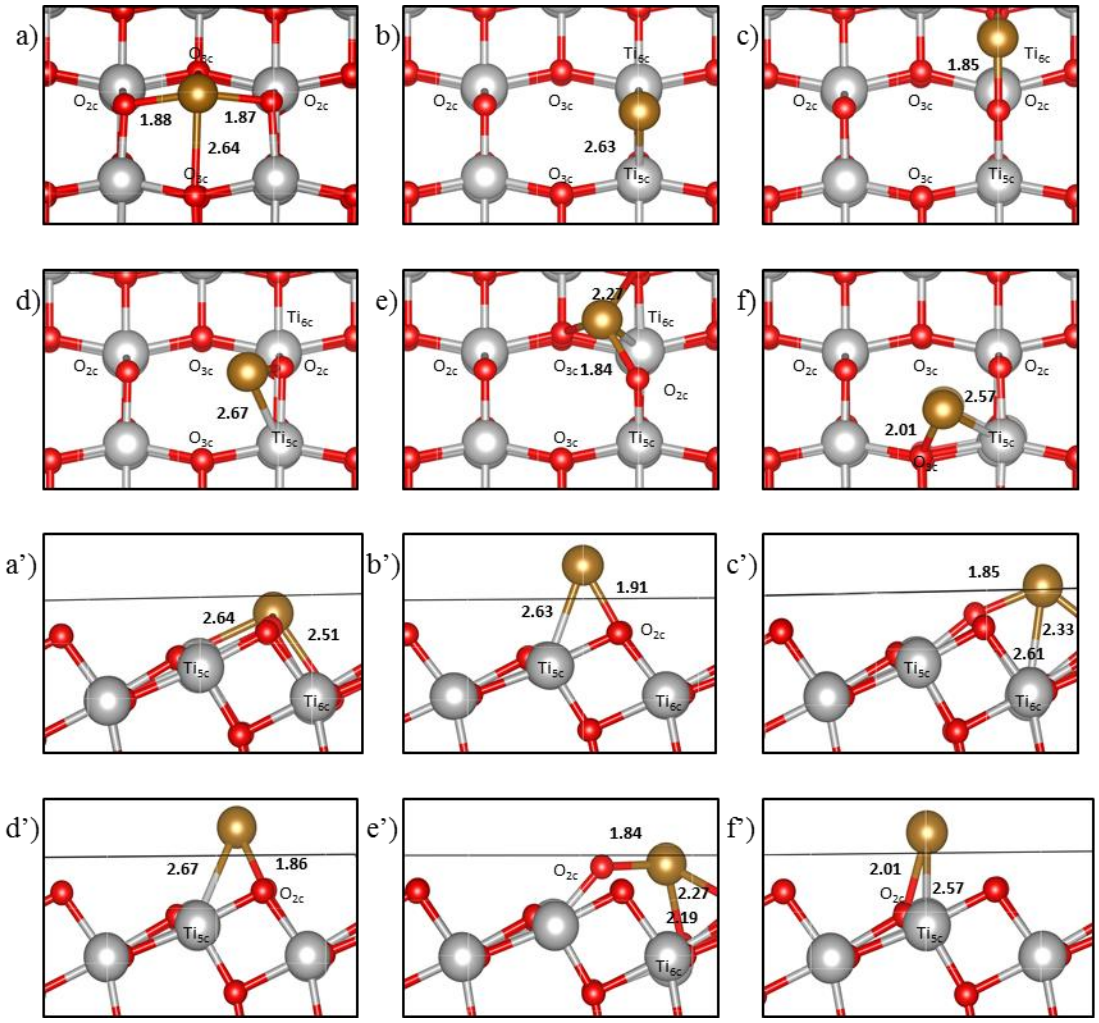

Figure S2: Top views of optimized geometries of a Cu adatom on Anatase TiO_2 (101) surface with bond lengths (in Angstroms): a) OO, b) OTi, c) OTiO. Rate determining transition state of d) Path 1, e) Path 2 and f) Path 3. The corresponding side views are shown in a'), b'), c'), d') e') and f').

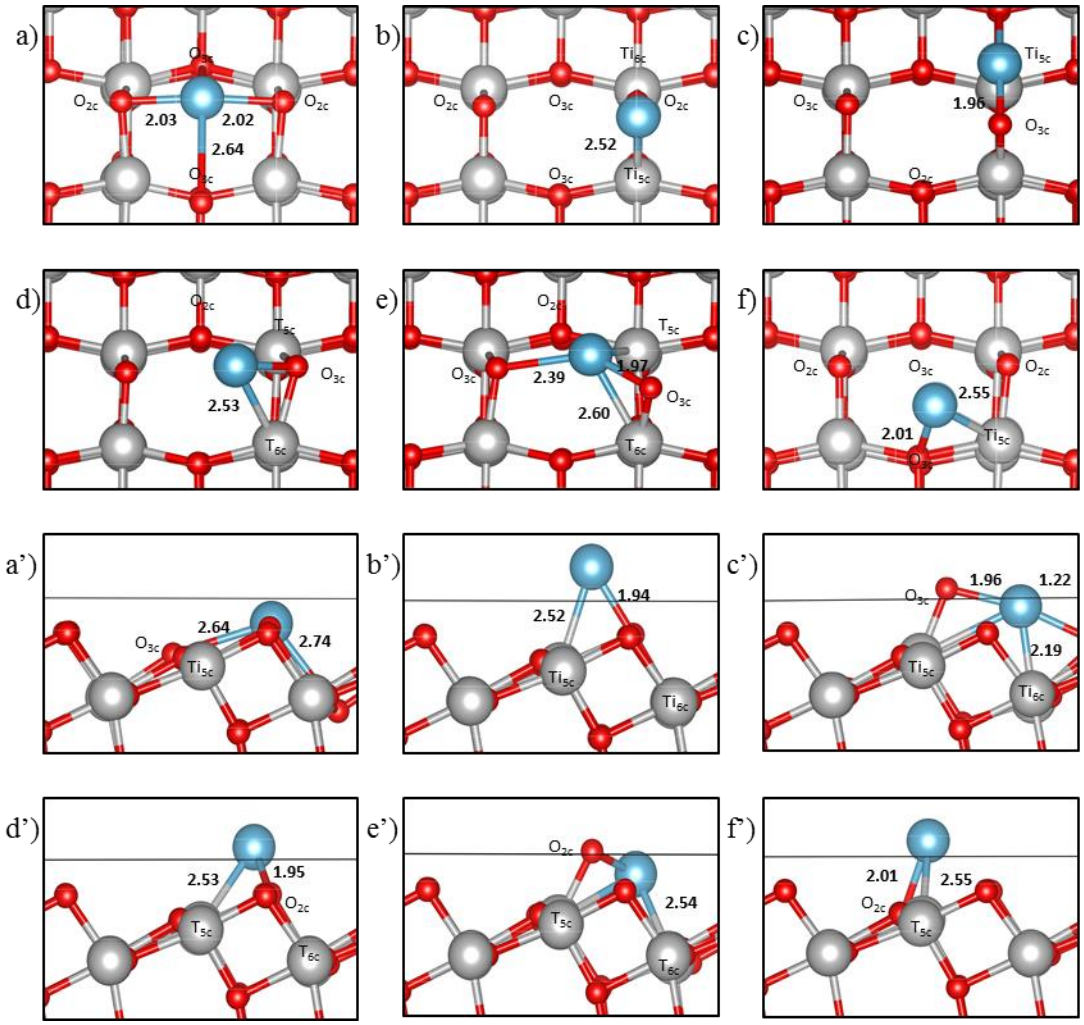

Figure S3: Top views of optimized geometries of a Pt adatom on Anatase TiO_2 (101) surface with bond lengths (in Angstroms): a) OO, b) OTi, c) OTiO. Rate determining transition state of d) Path 1, e) Path 2 and f) Path 3. The corresponding side views are shown in a'), b'), c'), d') e') and f').

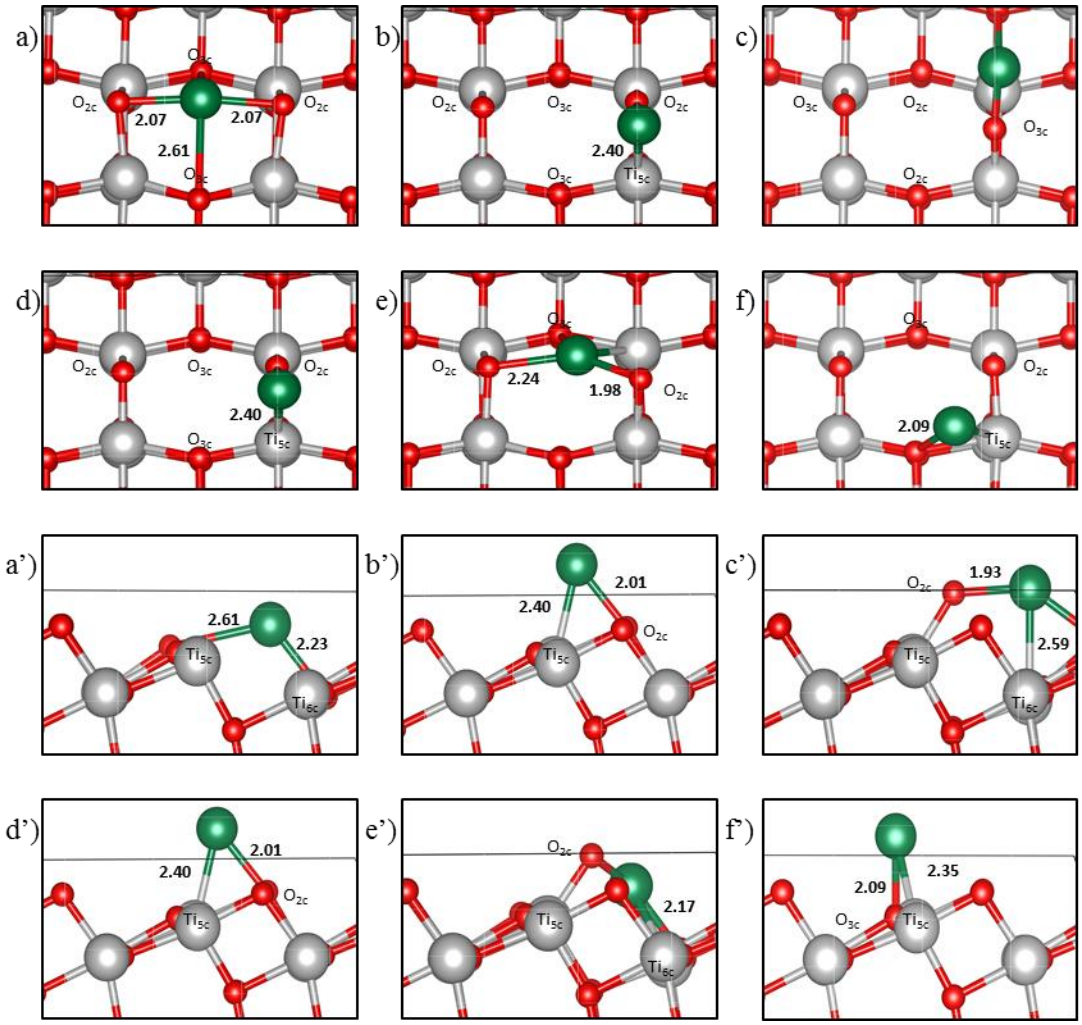

Figure S4: Top views of optimized geometries of a Rh adatom on Anatase TiO_2 (101) surface with bond lengths (in Angstroms): a) OO, b) OTi, c) OTiO. Rate determining transition state of d) Path 1, e) Path 2 and f) Path 3. The corresponding side views are shown in a'), b'), c'), d') e') and f').

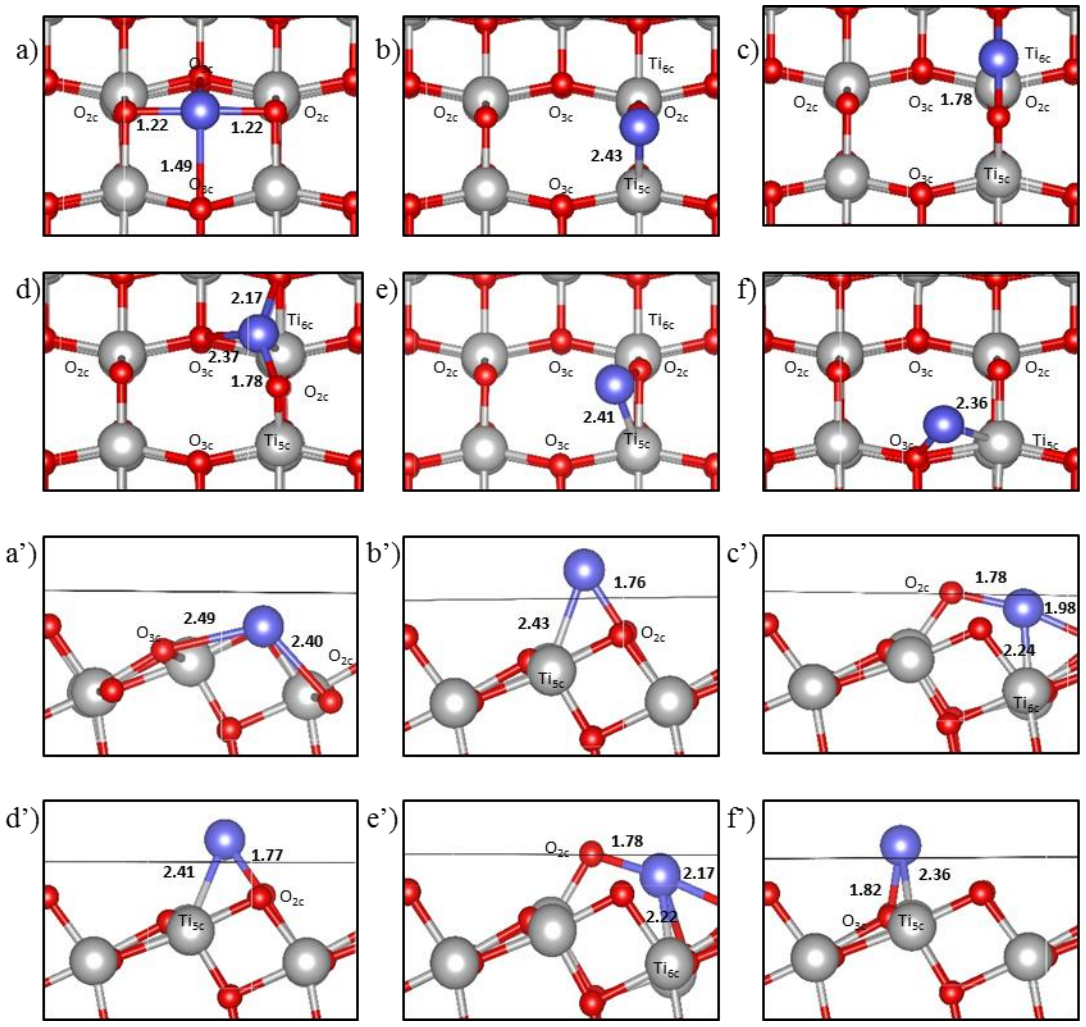

Figure S5: Top views of optimized geometries of a Ni adatom on Anatase TiO_2 (101) surface with bond lengths (in Angstroms): a) OO, b) OTi, c) OTiO. Rate determining transition state of d) Path 1, e) Path 2 and f) Path 3. The corresponding side views are shown in a'), b'), c'), d') e') and f').

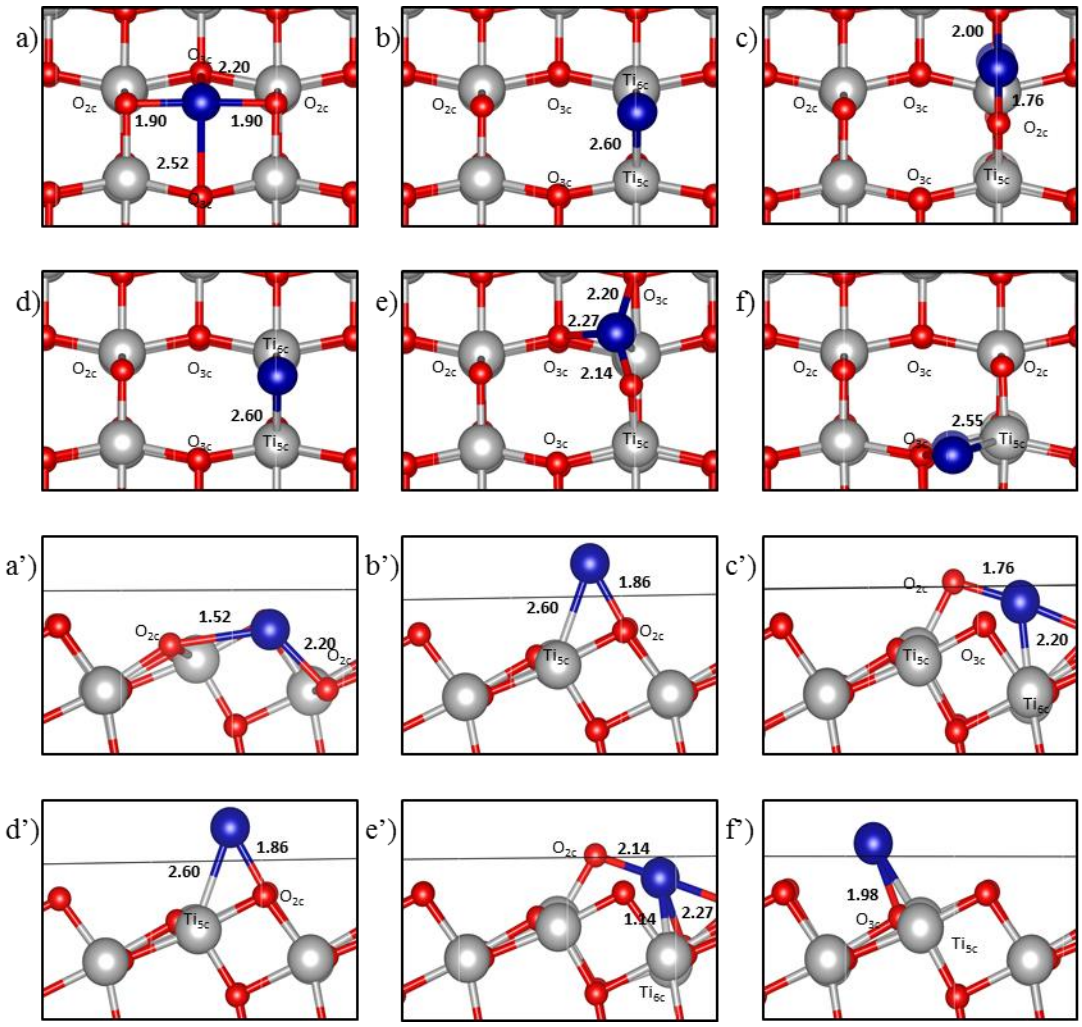

Figure S6: Top views of optimized geometries of a Co adatom on Anatase TiO_2 (101) surface with bond lengths (in Angstroms): a) OO, b) OTi, c) OTiO. Rate determining transition state of d) Path 1, e) Path 2 and f) Path 3. The corresponding side views are shown in a'), b'), c'), d') e') and f').

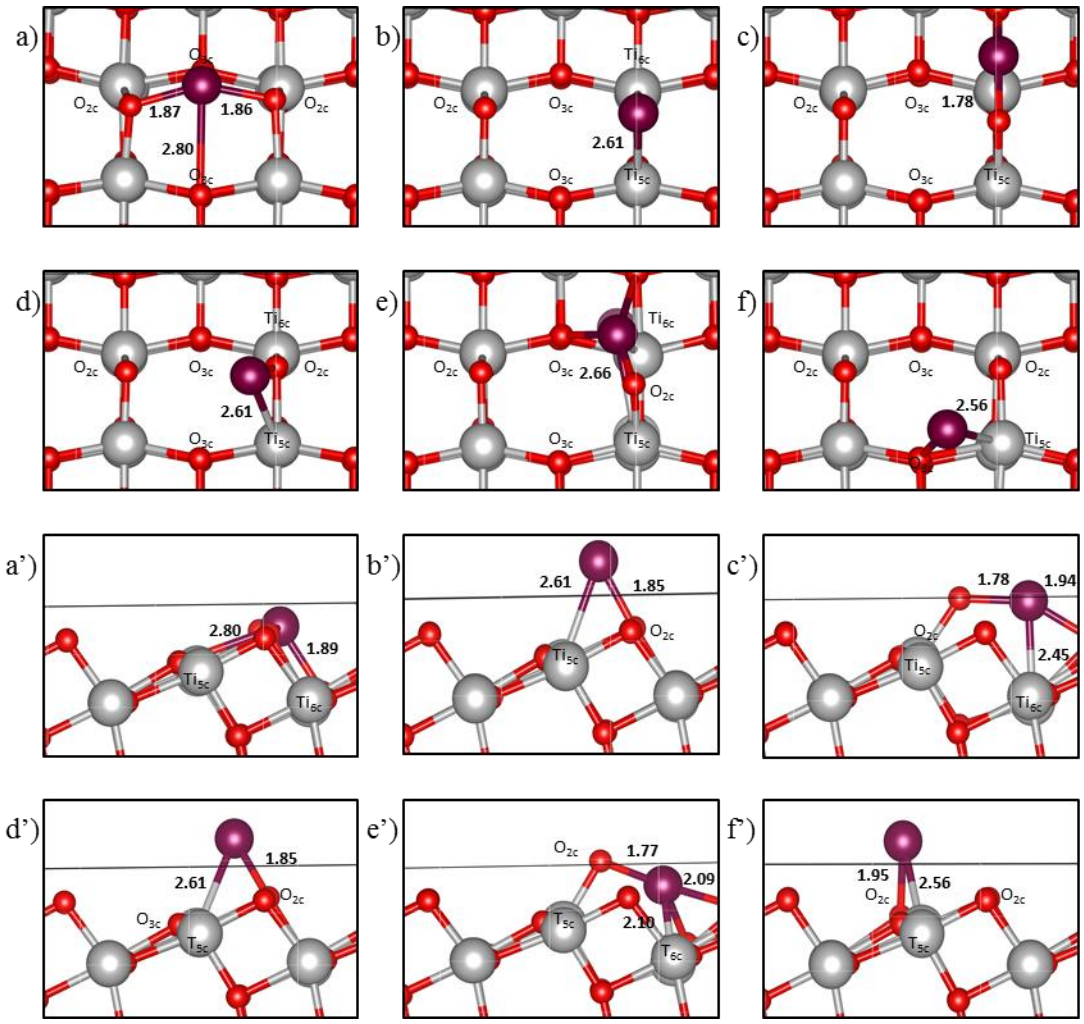

Figure S7: Top views of optimized geometries of a Fe adatom on Anatase TiO_2 (101) surface with bond lengths (in Angstroms): a) OO, b) OTi, c) OTiO. Rate determining transition state of d) Path 1, e) Path 2 and f) Path 3. The corresponding side views are shown in a'), b'), c'), d') e') and f').